PERFORMANCE OF HC AND HFC REFRIGERANTS IN A FINNED-TUBE EVAPORATOR AND ITS EFFECT ON SYSTEM EFFICIENCY

Domanski, P.A.,[*] Yashar, D. and Kim, M.
National Institute of Standards and Technology
Gaithersburg, MD 20899, USA

ABSTRACT

The paper presents a comparable evaluation of isobutane (R600a), propane (R290), R134a, R22, R410A, and R32 in an optimized finned-tube evaporator, and analyzes the impact of evaporator effects on the system coefficient of performance (COP). The study relied on a detailed evaporator model derived from NIST's EVAP-COND simulation package and used the ISHED1 scheme employing a non-Darwinian Learnable Evolution Model for circuitry optimization. In the process, 4500 circuitry designs were generated and evaluated for each refrigerant. The obtained evaporator optimization results were incorporated in a conventional analysis of the vapor compression cycle. For a theoretical cycle analysis without accounting for evaporator effects, the COP spread for the studied refrigerants was as high as 11.7 %. For cycle simulations including evaporator effects, the COP of R290 was better than that of R22 by up to 3.5 %, while the remaining refrigerants performed within approximately a 2 % COP band of the R22 baseline for the two condensing temperatures considered.

INTRODUCTION

Increasing concerns about climate change provides a new factor to a conventional system design striving for high efficiency and energy conservation at a given production cost. In addition to system optimization, the new factor is the preference - with other things being equal - to utilize refrigerants having a low Global Warming Potential (GWP). Although it has been recognized in several studies that the system's indirect contribution to climate change (carbon dioxide emissions from the fossil fuel power plant generating electricity to drive the system) is dominant for most applications, it is prudent to study and evaluate different fluids in a search for the optimal refrigerant for a given duty. The goal of this study was to evaluate the performance of R600a (isobutane), R290 (propane), R134a, R22, R410A, and R32 in an optimized finned-tube air-to-refrigerant evaporator and analyze its effect on the system coefficient of performance (COP).

Casson et al. (2002) presented a simulation study, in which they evaluated the performance of R22 alternatives in an optimized condenser and its effect on the system's efficiency. Their results showed that high-pressure refrigerants can be used more effectively with higher mass fluxes than R22 because of their small drop of saturation temperature for a given pressure drop. Their conclusions supported the results of Cavallini et al. (2000) who presented condensation heat transfer data for different fluids at the same so called Penalty Factor, which takes into account a refrigerant's saturation temperature drop during forced convection condensation.

---

[*]Corresponding author. National Institute of Standards and Technology, 100 Bureau Drive, Stop 8631, Gaithersburg, MD 20854-8631, tel: 301 975-5877; fax: 301 975-8973; email: piotr.domanski@nist.gov

Granryd and Palm (2003) investigated the optimum number of parallel sections in an evaporator, and presented their results in terms of a drop in refrigerant saturation temperature. They concluded that for optimum operation the drop of saturation temperature should be 33 % of the average temperature difference between the refrigerant and the tube wall, although the result was dependent on the used refrigerant heat transfer and pressure drop correlations.

REFRIGERANTS STUDIED
Table 1 presents the studied refrigerants in the order of their saturation vapor pressure corresponding to 7.0 °C dew-point temperature.

Table 1. Refrigerant information

Refrigerant	Saturated vapor pressure* kPa	Vapor density kg/m^3	Liquid density kg/m^3	Latent heat kJ/kg	Liquid conducti-vity W/(m·K)	Liquid viscosity µPa·s	dT_{sat}/dP K/kPa	ASHRAE (2000) safety designation	GWP (100 years)
isobutane	199.5	5.34	572.2	348.2	0.0958	183.05	0.1477	A3	20
R134a	374.6	18.32	1271.3	193.2	0.0889	243.88	0.0770	A1	1320
propane	584.4	12.69	519.0	364.5	0.1024	116.89	0.0585	A3	20
R22	621.5	26.35	1257.3	199.3	0.0916	200.13	0.0516	A1	1780
R410A	995.0	38.187	1141.7	212.6	0.1056	154.92	0.0329	A1/A1	2000
R32	1011.5	27.56	1030.6	304.0	0.1398	139.24	0.0322	A2	543

*Pressure corresponding to 7.0 °C saturation temperature.

The selected refrigerants have vastly different thermophysical properties. The vapor densities differ by a factor of five. If R22 is taken as a reference, the liquid conductivity, viscosity, and latent heat are different by as much as 52 %, 72 %, and 75 %, respectively. All refrigerant properties are based on REFPROP (Lemmon et al., 2002).

SIMULATION AND OPTIMIZATION TOOLS
In this study we used an evaporator simulation model EVAP from the EVAP-COND simulation package (NIST, 2003). Heat exchanger simulations by EVAP are organized in a tube-by-tube scheme allowing the user to specify arbitrary refrigerant circuitry architectures and a one-dimensional distribution of the inlet air. The program recognizes each tube as a separate entity for which it calculates heat transfer. When the refrigerant in a tube changes from two-phase to a superheated vapor, the model locates the transition point between the two phases in the tube and applies appropriate heat transfer and pressure drop correlations to the respective sections of the tube.

For the purpose of this study we examined and updated EVAP's refrigerant heat transfer and pressure drop correlations. From several good choices, we implemented the updated Kattan-Thome-Favrat correlation for the flow boiling heat transfer coefficient (Thome, 2003). For pressure drop calculations we chose the correlation by Müller-Steinhagen and Heck (1986). This correlation was rated as one of the top two out of seven correlations by Ould Didi et al. (2002) when checked against their 788 data points based on two tube diameters and five refrigerants, irrespective of the flow pattern. We also compared nine correlations against the predictions by the modified Pierre correlation (Choi et al., 2001), which was successfully applied to evaporation and condensation pressure drop data obtained from three independent

laboratories and covering seven refrigerants and two tube diameters. Figure 1 shows that the Müller-Steinhagen and Heck correlation agrees very well with the modified Pierre correlation. Compared to the Müller-Steinhagen and Heck correlation, the Pierre correlation has the disadvantage that it is not applicable to adiabatic flows. Also, the Pierre correlation calculates the overall pressure drop in a heat exchanger and cannot predict local pressure drop values, especially at high quality range approaching the saturated line.
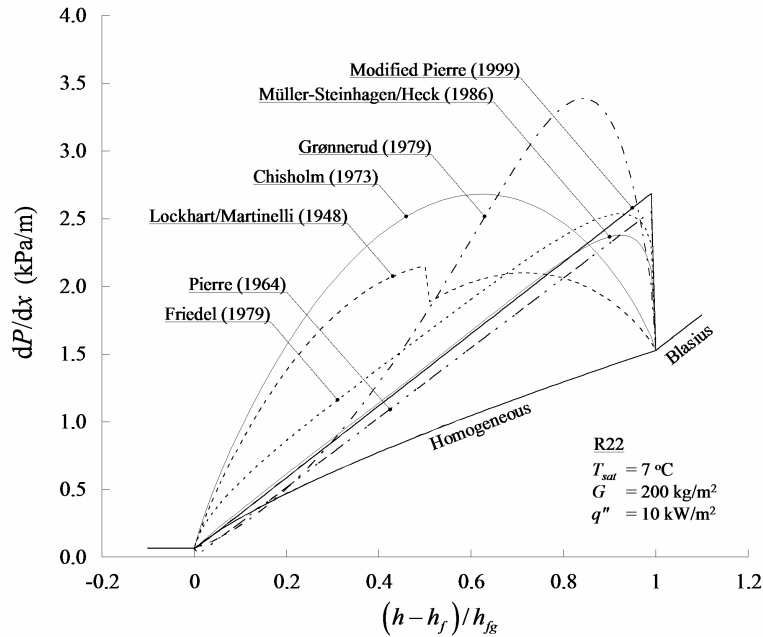
Figure 1. Comparison of nine pressure drop correlations

To obtain capacity predictions for an optimized evaporator for each refrigerant, we ran evaporator simulations using a novel optimization system called ISHED1 (Intelligent System for Heat Exchanger Design) (Domanski et al., 2004). It includes the evaporator model EVAP, the Control Module, and two modules: the Knowledge-based Evolutionary Computation Module and the Symbolic Learning-based Evolutionary Computation Module. These two modules guide the evolutionary process according to the concept referred to as the Learnable Evolution Model (LEM). The novelty of LEM methodology is that it combines a conventional evolution program with a non-Darwinian evolutionary computation employing symbolic learning.

Consistent with a conventional evolutionary computation approach, ISHED1 operates on one population (generation) of designs at a time. A population consists of a given number (determined by the user) of circuitry designs. Each member of the population is evaluated by EVAP, which simulates its performance and provides its cooling capacity as a single numerical fitness value. The designs and their fitness values are returned to the Control Module as an input for deriving the next generation of circuitry designs. Hence, the implemented process is a loop, and it is repeated for the number of populations specified by the user at the outset of the optimization run.

EVAPORATOR PERFORMANCE WITH SELECTED REFRIGERANTS

Table 2 shows the evaporator design data that was common for all evaporator simulations in this study. Additionally, the air condition was 26.7 °C dry-bulb temperature and 50 % relative humidity. The refrigerant inlet condition was specified in terms of the saturation temperature and subcooling at the inlet to the distributor, which was included in the simulation runs. With specified inlet parameters and environmental conditions, EVAP iterated refrigerant mass flow rate to arrive with a 5.0 K refrigerant exit superheat for the specified exit saturation temperature.

Table 2. Evaporator design information

Tube length	mm	500
Tube inside diameter	mm	9.2
Tube outside diameter	mm	10.0
Tube spacing	mm	25.4
Tube row spacing	mm	22.2
Number of tubes per row		12
Number of depth rows		3
Fin thickness	mm	0.2
Fin spacing	mm	2
Tube inner surface		smooth
Fin geometry		louver
Air volumetric flow rate	m³/min	25.5

The first simulation task was to obtain evaporator capacity for each refrigerant at the same exit saturation temperature of 7.0 °C. Because of significant differences in thermophysical properties, refrigerant circuitry had to be optimized for each refrigerant. We started by manually developing five basic circuitry architectures involving 1, 1.5, 2, 3, and 4 circuits, four of which are shown in Figure 2. Then we used ISHED1 for further refrigerant circuitry optimization with the input of 300 populations and 15 members per a population. The 1.5, 2, 3, and 4-circuit designs were included as "seed" designs in the first population. The remaining 11 designs of this population were developed by ISHED1. In total, each optimization run included 4500 calls to EVAP.
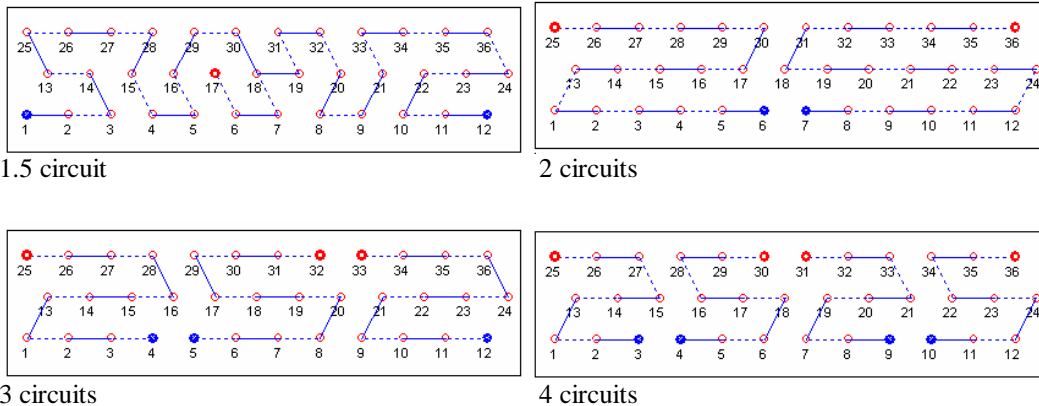

Figure 2. Manually developed 1.5, 2, 3, and 4 circuit designs (side view; circles denote tubes; continuous lines indicate return bends on the near side of the heat exchanger, broken lines indicate return bends on the far side, full circles indicate outlet tubes).

Figure 3 presents capacity results for the prearranged 1, 1.5, 2, 3, 4 circuit designs and the optimized designs developed by ISHED1. For each refrigerant, the design developed by ISHED1 outperformed the best of the prearranged designs. For R32, R410A, R290, and R22, ISHED1 developed individually optimized designs which were based on a 1.5 circuit. Although each of these designs had a somewhat different layout, EVAP simulations confirmed that they were equivalent in performance. For this reason, only the R410A 1.5-circuitry ISHED1-developed design was used further for R32, R410A, R290, and R22

(shown in Figure 4). For R134a and R600a, a 3-circuit and a 4-circuit design, respectively, were proposed by ISHED1.
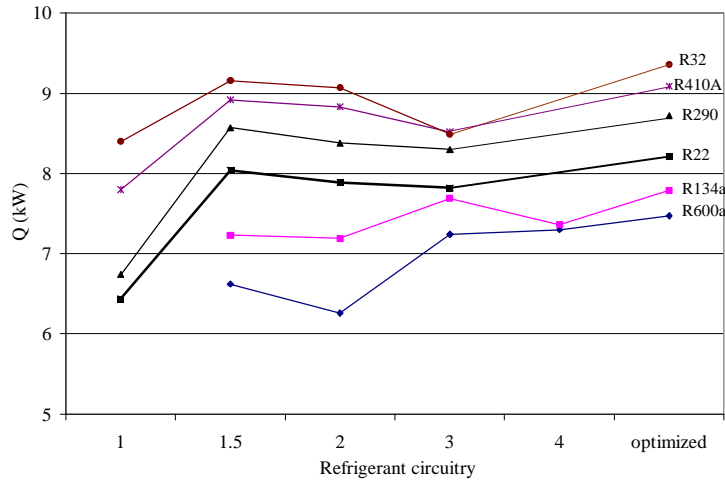

Figure 3. Evaporator capacities for manually developed and ISHED1-optimized circuitry designs
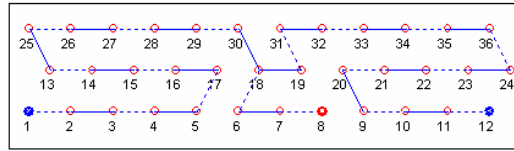

Figure 4. 1.5-circuit design optimized for R410A by ISHED1

EVAP simulations using ISHED1 optimized evaporators generated results presented in Table 3. For comparative evaluation, we selected R22 as our reference. R600a had the lowest capacity, 9.5 % below that of R22, and R32 had the highest capacity exceeding that of R22 by 14.5 %. We also should note that the low-pressure refrigerants, R600a and R134a, had the lowest ratio of the latent capacity to total capacity.

Table 3. Summary of simulation results for ISHED1-optimized designs for $T_{sat} = 7.0$ ℃

Refrigerant	Number of circuits	Refrig. inlet quality	Refrig. outlet pressure	Refrig. pressure drop	Refrig. sat. temp. drop	Refrig. mass flow rate	Q	Q_l/Q	Q/Q_{R22}
		(-)	kPa	kPa	K	kg/h	kW		
R600a	4	0.26	200	12	1.7	102.0	7.43	0.18	0.905
R134a	3	0.27	375	27	2.0	195.6	7.787	0.20	0.948
R290	1.5	0.27	585	59	2.8	116.1	8.706	0.23	1.060
R22	**1.5**	**0.23**	**621**	**64**	**3.2**	**190.7**	**8.211**	**0.21**	**1.000**
R410A	1.5	0.29	993	57	1.8	213.5	9.091	0.25	1.107
R32	1.5	0.24	1012	40	1.3	143.0	9.399	0.26	1.145

IMPACT OF EVAPORATOR PERFORMANCE ON SYSTEM COP

We used the basic thermodynamic analysis of the vapor compression cycle, as implemented by the CYCLE_D model (Domanski et al., 2003), to assess the impact that the evaporator performance for different refrigerants has on the COP. In the CYCLE_D simulations, refrigerant saturation temperatures in the evaporator and condenser are specified as input. To acquire all of the data, we performed two rounds of simulations. In the first round, we used the same evaporator exit saturation temperature, T_{sat}, of 7.0 °C for each refrigerant. For the second round, we first performed iterative EVAP simulations at various evaporator saturation temperatures to obtain a capacity equal to that of R22 at 7.0 °C saturation temperature. The obtained saturation temperatures, constituted a new input for each refrigerant (instead of 7.0 °C) for the second round of CYCLE_D simulations.

All CYCLE_D simulations were performed at two condensing temperatures of 38.0 °C and 45.0 °C. Table 4 contains the additional CYCLE_D input used in these calculations. Table 5 presents the obtained results for the two rounds of simulations. The results in the left-hand-side of the table, with T_{sat}=7.0 °C, are from the basic thermodynamic calculations of the cycle. The results located in the right-hand-side of the table, with different values of T_{sat}, account for the impact that the thermodynamic and transport properties have on the cycle through their effect on the performance of the optimized evaporator.

Table 4. Input data to CYCLE_D

Compressor isentropic efficiency	.65
Compressor volumetric efficiency	.82
Electric motor efficiency	.85
Suction line pressure drop (°C of sat. temp)	1.0 °C
Discharge line pressure drop (°C of sat. temp)	1.0 °C
Evaporator superheat	5.0 °C
Condenser subcooling	5.0 °C
LL-SL heat exchanger	none

Table 5. Performance for the theoretical cycle and the cycle accounting for evaporator effects

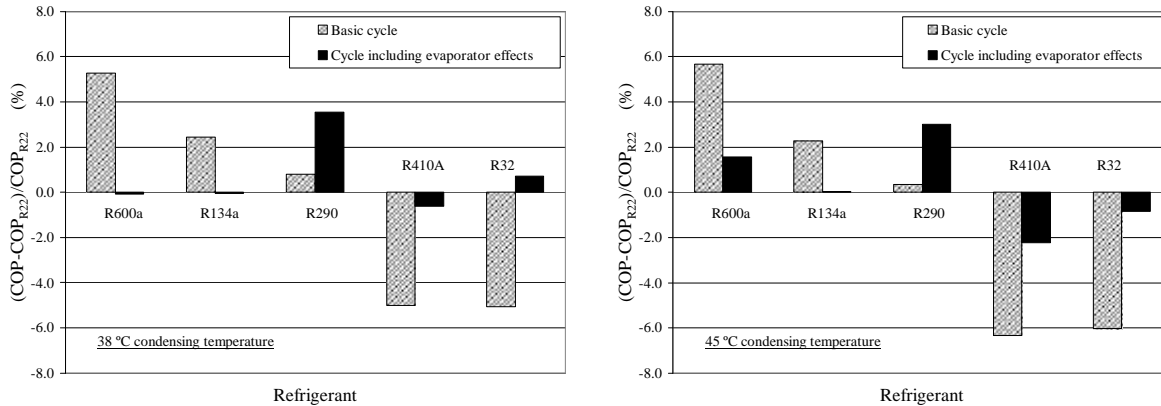| 38.0 °C Condensing temperature							
Refrigerant	T_{sat} (°C)	COP	(COP-COP$_{R22}$) /COP$_{R22}$ (%)	T_{sat} (°C)	COP	(COP-COP$_{R22}$) /COP$_{R22}$ (%)	Q_l/Q
R600a	7.0	4.103	5.3	5.7	3.895	-0.1	0.22
R134a	7.0	3.993	2.4	6.4	3.896	-0.1	0.22
R290	7.0	3.929	0.8	7.7	4.036	3.5	0.21
R22	**7.0**	**3.898**	**0.0**	**7.0**	**3.898**	**0.0**	**0.21**
R410A	7.0	3.703	-5.0	8.1	3.874	-0.6	0.21
R32	7.0	3.701	-5.1	8.5	3.926	0.7	0.21
45.0 °C Condensing temperature							
Refrigerant	T_{sat} (°C)	COP	(COP-COP$_{R22}$) /COP$_{R22}$ (%)	T_{sat} (°C)	COP	(COP-COP$_{R22}$) /COP$_{R22}$ (%)	Q_l/Q
R600a	7.0	3.237	5.7	5.8	3.111	1.6	0.22
R134a	7.0	3.133	2.3	6.4	3.064	0.0	0.22
R290	7.0	3.074	0.4	7.8	3.155	3.0	0.21
R22	**7.0**	**3.063**	**0.0**	**7.0**	**3.063**	**0.0**	**0.21**
R410A	7.0	2.869	-6.3	8.2	2.995	-2.2	0.21
R32	7.0	2.878	-6.0	8.5	3.073	-0.8	0.21

Figure 5. COPs compared to the COP of R22 for the basic cycle and for the cycle including evaporator effects for 38.0 ℃ and 45.0 ° condensing temperatures

Figure 5 presents COP results referenced to the COP of the baseline R22 cycle. It is seen in the figure generated for the 38.0 ℃ condensing temperature that the theoretical simulations for the basic cycle ranked these refrigerants in the reverse order of their pressure in the evaporator, with COP of R600a being 5.3 % better than that of R22, and the COP of R32 being 5.1 % worse. It is interesting to notice that the performance of the group was found to be much more uniform when the effects of the optimized evaporators and corresponding saturation temperatures are included in the simulations. While propane arrived as the most efficient refrigerant with a 3.5 % better COP than R22, the COPs of the remaining refrigerants were found to be within -0.6 % to 0.7 % of the COP of R22. The high-pressure R32 experienced the greatest COP improvement when evaporator effects were taken into account, and in relation to R600a it changed the 10.4 % COP deficit to 0.8 % advantage. All refrigerant provided similar latent capacities. The results for the 45.0 ℃ condensing temperature display similar trends with the difference that the high-pressure refrigerants showed somewhat lower performance because the cycle moved closer to their critical points.

CONCLUDING REMARKS
This study evaluated the performance of R600a, R134a, R290, R22, R410A, and R32 in an optimized evaporator and its impact on the system COP. The evaporator optimization search used a non-Darwinian evolutionary scheme, which evaluated 4500 refrigerant circuitry designs for each refrigerant studied. For a 7.0 ℃ evaporator exit saturation temperature, and using R22 as a reference, R32, R410A, and R290, had a greater capacity by 14.5 %, 10.7 %, and 6.0 %, while R134a and R690a had a lower capacity by 5.2 % and 9.5 %, respectively. The subsequent cycle simulations with a 7.0 ℃ evaporator exit saturation temperature showed the COPs of the studied refrigerants to be in the reverse order of their evaporator pressure. For the simulations including evaporator effects (performed at a different saturation temperature for each fluid to match the R22 capacity), the COP of R290 was better than that of R22 by approximately 3 %, while the remaining refrigerants performed within approximately a 2 % band of the R22 COP baseline for the two condensing temperatures used. R32 overcame the 10 % COP deficit it had in the basic cycle in reference to R600a and showed a comparable performance when evaporator effects were included in the cycle simulation. Hence, the high-pressure refrigerants (with a low critical temperature) tend to have a lower COP than the low-pressure refrigerants, however, the high-pressure refrigerants tend to perform better in finned tube evaporators, and this effect mitigates their theoretical COP disadvantage.

It must be emphasized that this study considered only the evaporator effects, and did not include similar effects that may be introduced by the condenser. Also, we have to note that selection of the compressor and relative sizing of the remaining components will affect the performance of a complete system. This study was not concerned with design tradeoffs and the cost related to the practical implementation of different refrigerants, e.g., safety considerations for flammable refrigerants, equipment size, pressure, or lubricant issues.

NOMENCLATURE

COP - coefficient of performance
G - refrigerant mass flux $(kg/(s \cdot m^2))$
GWP - Global Warming Potential
h - enthalpy (kJ/kg)
h_{fg} - latent heat (kJ/kg)
h_f - enthalpy of sat. liquid (kJ/kg)
P - pressure (kPa)

Q - total capacity (kW)
Q_l - latent capacity, portion of total capacity due to water vapor removal (kW)
T_{sat} - sat. temperature at the evaporator exit (ºC)
x - vapor quality (-)

REFERENCES

Casson, V., Cavallini, A., Cecchinato, L., Del Col, D., Doretti, L., Fornasieru, E., Rossetto, L., Zilio, C. (2002), "Performance of Finned Coil Condensers Optimized for New HFC Refrigerants"/*ASHRAE Trans*., ASHRAE Summer Mtg., paper HI-02-1-3.

Cavallini, A., Del Col, D., Doretti, L., Rossetto, L. (2000), "Condensation Heat Transfer of New Refrigerants: Advantages of High Pressure Fluids"/*Eighth Int. Refrig. Conf. at Purdue University*, West Laffayette, IN, USA.

Granryd, E., Palm, B. (2003), "Optimum Number of Parallel Sections in Evaporators"/*Int. Congress. Refrig*., paper ICR0077.

ASHRAE (2001), "Designation and Safety Classification of Refrigerants; ANSI/ASHRAE Standard 34-2001"/*ASHRAE*. Atlanta, GA, USA.

NIST, 2003, "EVAP-COND, Simulation models for finned-tube heat exchangers"/ *National Institute of Standards and Technology*, Gaithersburg, MD, USA. http://www2.bfrl.nist.gov/software/evap-cond/

Thome, J.R., (2003), "Update on the Kattan-Thome-Favrat Flow Boiling Model and Flow Pattern Map"/*Int. J.Heat and Fluids Flow*, submitted for publication.

Ould Didi, M.B., Kattan, N., Thome, J.R. (2002), "Prediction of two-phase pressure gradients of refrigerants in horizontal tubes"/*Int. J. Refrig.,* Vol. 25, pp. 935-947.

Müller-Steinhagen, H. and Heck, K. (1986), "A Simple Friction Pressure Drop Correlation For Two-Phase Flow In Pipes"/Chem. Eng. Process., Vol. 20, pp. 297-308.

Choi, J.Y., Kedzierski, M.A., Domanski, P.A. (2001), "Generalized Pressure Drop Correlation for Evaporation and Condensation In Smooth and Micro-fin Tubes"/*IIR Commission B1 Conference, Thermophysical Properties and Transfer Processes of New Refrigerants*, October 3-5, Paderborn, Germany.

Domanski, P.A., Yashar, D., Kaufman, K.A., and Michalski, R.S., (2004), "Optimized Design of Finned-Tube Evaporators Using Learnable Evolution Methods", *Int. J. of HVAC&R Research*, Vol. 10, No. 2, pp. 201-212.

Lemmon, E.W., McLinden, M.O., Huber, M.L. (2002), "NIST Reference Fluids Thermo-dynamic and Transport Properties-REFPROP"/*National Institute of Standards and Technology*, NIST Standard Reference Database 23, Ver. 7. Gaithersburg, MD, USA.

Domanski, P.A., Didion, D.A., Chi, J. (2003). "CYCLE_D: NIST Vapor Compression Cycle Design Program"/*National Institute of Standards and Technology*, NIST Standard Reference Database 49, Ver. 3, Gaithersburg, MD, USA.